Respiratory Physiology & Neurobiology 266 (2019) 9–17

Contents lists available at ScienceDirect

Respiratory Physiology & Neurobiology

journal homepage: www.elsevier.com/locate/resphysiol

Cigarette smoke exposure combined with lipopolysaccharides induced pulmonary fibrosis in mice

Lijuan Fang[a], Qingmei Cheng[a], Feiyan Zhao[a], Haipeng Cheng[a], Yongyu Luo[a], Xingwen Bao[a], Yanghang Li[a], Xinyue Liang[a], Yanhong Huang[a], Jianping Xu[a], Jianzhong Han[a], Yiting Tang[a], Siyuan Tang[b], Wei Liu[b], Ziqiang Luo[a], DanDan Feng[a,*]

[a] Department of Physiology, Xiangya School of Medicine, Central South University, Changsha, Hunan, China
[b] Xiangya Nursing School, Central South University, Changsha, Hunan, China

ARTICLE INFO

Keywords:
Pulmonary fibrosis
Cigarette smoke
Lipopolysaccharide
Collagen deposition
Inflammatory cytokine

ABSTRACT

Cigarette smoke (CS) is a risk factor for pulmonary fibrosis and lipopolysaccharides (LPS) are associated with human occupational lung diseases; however, their combined role in pulmonary fibrosis remains unknown. Therefore, we investigated whether CS combined with LPS induces pulmonary fibrosis in mice. C57BL/6 mice were exposed to CS or normal air for 21 or 35 days, followed by LPS or saline instillation on day 14, 21, and 28. Lung function was tested, and lung tissues were harvested for histological and molecular analyses. Compared to the control, CS and LPS groups, the CS + LPS group showed reduced body weight and survival rate, increased respiratory resistance, decreased lung compliance, marked alveolar structure destruction, and fibrotic lesion formation. Lung tissues showed a considerable increase in IL-6, TNF-α, IL-1β, α-SMA, and TGF-β levels and collagen content. Our results indicate that cigarette smoke exposure followed by LPS in mice induces pulmonary fibrosis with pathophysiology consistent with that of human pulmonary fibrosis.

1. Introduction

Pulmonary fibrosis is a chronic, progressive, and irreversible lung-restricted disease. It is the most common outcome of interstitial lung disease (Liu et al., 2016), which is characterized by alveolar epithelial cell damage and hyperplasia, accumulation of inflammatory cells, fibroblast hyperplasia, extracellular matrix deposition, and scar formation (Moore and Hogaboam, 2008).

The aetiology of pulmonary fibrosis is complex, and it is believed to be caused by genetic and various environmental factors such as tobacco smoke, metal, drugs, and contact with infectious substances (King et al., 2011; Raghu et al., 2011; Selman and Pardo, 2014). It is well known that cigarette smoking induces chronic obstructive pulmonary disease (COPD), and in some heavy smokers, COPD disease manifests as both pulmonary emphysema (upper lobe of the lung) and pulmonary fibrosis (lower lobe of the lung) (Cottin et al., 2005; Grubstein et al., 2005). Smoking is also believed to be a high-risk factor for pulmonary fibrosis, and smoking-induced pulmonary epithelial cell injury may persist for several years even after quitting smoking (Baumgartner et al., 1997). Such epithelial cell damage plays a key role in the activation of fibrogenesis, thereby contributing to the pathogenesis of pulmonary fibrosis. In vivo studies have shown that nicotine directly affects the ionic homeostasis of lung epithelial cells and provokes an inflammatory response that contributes to cellular damage (Roomans et al., 2002; Jensen et al., 2012).

Lipopolysaccharides (LPS) are important cell wall components in gram-negative bacteria. LPS are ubiquitous in the environment and associated with many human occupational lung diseases, most of which are associated with organic dust exposure (Thorn, 2001). LPS promote the activation and aggregation of inflammatory cells and the production and release of other inflammatory mediators, resulting in diffuse lung tissue damage (Maniatis et al., 2008; Sebai et al., 2009).

LPS activate the mononuclear macrophage system to produce a several fibrogenic cytokines such as transforming growth factor beta 1 (TGF-β1), which act on pulmonary fibroblasts via different direct or indirect pathways (Olman et al., 2004). Following this LPS-induced damage, the fibroblasts induce chemotaxis and activate pulmonary macrophages through inflammatory factors such as interleukin-6 (IL-6), thus participating in the lung fibrosis process with other cells (Vancheri et al., 1996; Seki et al., 2007). In fact, it has been confirmed that LPS directly activate fibroblasts and promote collagen synthesis and secretion, eventually causing diffuse interstitial pulmonary fibrosis (He et al.,

* Corresponding author.
E-mail address: fengdandan@csu.edu.cn (D. Feng).

https://doi.org/10.1016/j.resp.2019.04.010
Received 20 December 2018; Received in revised form 31 March 2019; Accepted 21 April 2019
Available online 22 April 2019

2009). Furthermore, rapid pulmonary fibrosis could be induced by acute lung injury via the LPS three-hit regimen (Li et al., 2009; He et al., 2010).

It is known that LPS are associated with many occupational lung diseases in humans and that smoking is a high-risk factor for the development of pulmonary fibrosis. However, there is no direct evidence to show the strong link between smoke exposure and pulmonary fibrosis in patients with LPS-induced lung injury. Therefore, in this study, we investigated pulmonary fibrosis in mice exposed to cigarette smoke and subjected to LPS-induced lung injury. This study provides a theoretical foundation for the development of animal models for investigating and testing novel approaches for the clinical treatment of pulmonary fibrosis.

2. Material and methods

2.1. Experimental animals

Male C57BL/6 mice aged 8–10 weeks (weighing 20–25 g) were purchased from the Animal Center of Central South University, Changsha, China. The mice were housed in a controlled environment: 22℃ temperature, 12:12 h light/dark cycle, and ad libitum access to food and water. All in vivo experimental protocols were approved by the local Ethics Committee and were performed strictly in accordance with the NIH Guide for the Care and Use of Laboratory Animals.

The mice were randomly divided into four groups (n = 8–15 per group): (1) Control: Norm + intratracheal saline injection of saline; (2) CS: cigarette smoke exposure; (3) LPS: intratracheal LPS injection; and (4) CS + LPS: intratracheal LPS injection + cigarette smoke exposure.

The commercial filtered cigarettes (Xiangsiniao from the Hunan Tobacco Industrial Co., Ltd., China), characterized by smoke containing 11 mg tar, 13 mg carbon monoxide, and 0.9 mg nicotine per cigarette, were used in this study. Mice in the CS and CS + LPS groups were placed in a Plexiglass whole-body exposure chamber (60 × 60 × 70 cm) and exposed to successive periods of cigarette smoke for 2 h/day for 7 days/week. The animals were sacrificed under anaesthesia at D35.

The amount of cigarette was increased as showed in Fig. 1. To allow adaptation, mice were exposed to gradually increasing concentration of smoke. First, mice habituated for 7 days with 6 cigarettes a day, and then were successively exposed to 8 or 10 cigarettes until the end of the study.

At D14, D21, and D28, 0.9 mg/kg LPS (Sigma, USA) was administered in 50 μL saline by direct tracheal instillation. High LPS dose is usually used in acute lung injury animal models, and the objective of this study was to observe inflammatory factor-mediated pulmonary fibrosis induced by cigarette smoke exposure; therefore, a relatively low LPS dose was adopted in this study.

The particle concentration (mg/m^3) in the exposure chamber was measured by a medium-flow intelligent dust sampler (Qingdao Lubo Environmental Technology Co., Ltd, China), and the carboxyhaemoglobin (HbCO) level was determined by spectrophotometry (Table 1).

Table 1
Particle concentration and HbCO level.

Amount of cigarettes	Particle concentration (mg/m^3, mean ± SEM)	HbCO level(%, mean ± SEM)	
		0 h after CS exposure	24 h after CS exposure
6	170.78 ± 4.88	27.91 ± 1.85	4.32 ± 1.23
8	206.71 ± 7.30	40.45 ± 2.63	6.45 ± 1.56
10	258.78 ± 8.21	47.95 ± 2.34	7.95 ± 1.41

2.2. Measurement of dynamic lung compliance (Cdyn) and airway respiratory resistance (RL)

To determine the effect of cigarette exposure and LPS injections on lung function, we tested Cdyn (ml/cmH2O) and RL (cmH2O·s/ml) using the pulmonary function equipment from Buxco Research Systems (Buxco, USA).

2.3. Pathological changes in lung tissue

Animals were sacrificed under anaesthesia, and the lung tissues were collected. For morphometric analysis, the right upper lobe tissues from non-lavaged lungs were harvested and fixed in 4% paraformaldehyde for at least 24 h and embedded in paraffin. Five-micron-thick sections were cut and stained with haematoxylin/eosin and Masson's trichrome according to standard methods and then examined under a light microscope. The degree of alveolar inflammation was evaluated by methods previously described by Szapiel et al. (1979), and the severity of pulmonary fibrosis was evaluated in terms of the Ashcroft score (Ashcroft et al., 1988). Details about the evaluation of degree of alveolar inflammation and pulmonary fibrosis are provided in Tables 2 and 3.

2.4. Lung hydroxyproline assays

Hydroxyproline is a collagen-specific amino acid and is one of the main components of collagen. Therefore, the lung collagen content was estimated by measuring the hydroxyproline levels (Akhmetshina et al., 2012; Dohi et al., 2000). Hydroxyproline content was measured using a hydroxyproline detection kit (Jiancheng Biotechnology Institute, Nanjing, China) according to the manufacturer's protocol. Absorbance at 550 nm was measured using Microplate Reader (Thermo Fisher Scientific, USA), and hydroxyproline content was calculated per the kit manufacturer's instructions.

2.5. ELISA for cytokine measurements

The lungs were homogenized in phosphate-buffered saline (PBS, pH 7.4) containing protease inhibitors (Roche Applied Sciences, Germany) and centrifuged at 10,000 ×*g* to remove insoluble debris. IL-1β, TNF-α, and IL-6 levels in the lung tissue homogenate were determined using the respective mouse ELISA kits (Invitrogen, USA), according to the

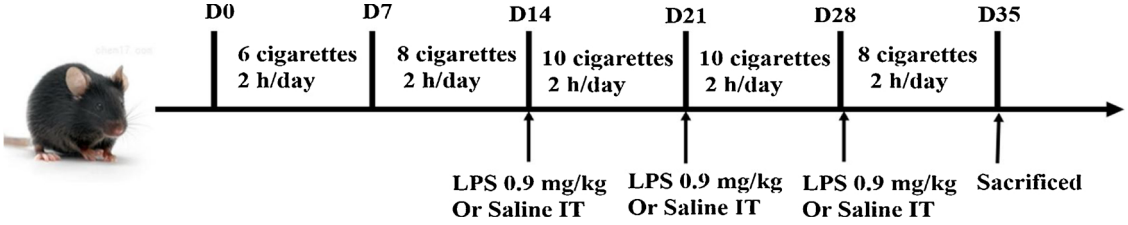

Fig. 1. A schematic depicting the smoke exposure protocol. Mice were exposed to room air or increasing concentrations of cigarette smoke during the study period. Then, the mice were subjected to tracheal instillation of LPS or saline on the indicated days. At D35, the mice were sacrificed, and lung samples were collected for further analysis.

Table 2
Criteria for grading alveolar inflammation.

Grade of alveolitis	Histological features
0	No alveolitis occurred
1	Mild alveolitis, alveolar septum widened slightly, mononuclear cell infiltration and adjacent to the pleura or localized, lesion size less than 20%, without alveolar structure destruction
2	Moderate alveolitis, the lesion ranges from 20% to 50% and is relatively severe near the pleura
3	Severe alveolitis with diffuse distribution, the lesion range is more than 50%, occasionally lung consolidation is seen

Table 3
Criteria for grading pulmonary fibrosis.

Grade of fibrosis	Histological features
0	Normal lung
1	Minimal fibrous thickening of alveolar or bronchiolar walls
2*	
3	Moderate thickening of walls without obvious damage to lung architecture
4*	
5	Increased fibrosis with definite damage to lung structure and formation of fibrous bands or small fibrous masses
6*	
7	Severe distortion of structure and large fibrous areas; "honeycomb lung" is placed in this category
8	Total fibrous obliteration of the field

* the severity is between the former and the latter.

manufacturers' protocols.

2.6. Western blot analysis

Protein lysates from lung tissues were prepared in RIPA lysis buffer plus protease inhibitor cocktail, and the total protein concentration was determined using the Pierce™ BCA Protein Assay Kit (Thermo Fisher Scientific, USA). The proteins were then separated by 10% sodium dodecyl sulphate-polyacrylamide gel electrophoresis (SDS-PAGE) and transferred to a polyvinylidene fluoride (PVDF) membrane (Millipore, USA). After blocking with 5% non-fat powdered milk diluted in Tris-buffered saline containing 0.1% Tween-20 (1X TBST), the membranes were incubated overnight at 4 °C with primary antibodies against β-actin (Sigma), GAPDH (Yeasen, China), TGF-β (Santa Cruz Biotechnology Inc., USA), α-SMA (Proteintech, China), and Collagen III (Cell Signaling Technology, USA). The membranes were washed three times (10 min per wash) with 1X TBST buffer and incubated with horseradish peroxidase-conjugated secondary antibody for 2 h at room temperature. Immunoreactive bands were detected using chemiluminescence reagents (Millipore, USA) and the Molecular Imager ChemiDoc XRS System (Bio-Rad, USA). The abundance of the targeted protein was analysed using the ImageJ software. All the experiments were repeated three times.

2.7. Reverse transcription-quantitative polymerase chain reaction (RT-qPCR) analysis

Total RNA was extracted from lung tissues with TRIzol reagent (Takara, Japan) and was reverse transcribed into cDNA using a PrimeScript RT reagent Kit (Takara, Japan), following the manufacturer's instructions. RT-qPCR was performed using the CFX96 Touch real-time PCR detection system (Bio-Rad). The primers used have been listed in Table 4.

2.8. Immunohistochemistry

Paraffin sections were deparaffinized, dehydrated, and incubated with 3% hydrogen peroxide to block endogenous peroxidase activity. Then, the sections were incubated with a blocking buffer to block nonspecific staining and incubated overnight at 4℃ with an α-SMA antibody (Abcam, USA). Subsequently, the sections were incubated with the secondary antibody at 37℃ for 1 h, followed by incubation with 0.05% diaminobenzidine. The sections were counterstained, rinsed with PBS to terminate the reaction, and protected with coverslips before microscopic examination.

2.9. Statistical analysis

All data were tested for normal distribution. The normally distributed data were presented as mean ± SEM, and one-way ANOVA was used for statistical analysis. Other data were described as median and inter-quartile range, and a nonparametric test (Kruskal-Wallis test) was applied. Survival rates were evaluated with a log-rank test over a period of 35 days. GraphPad Prism software was used for all analyses. Differences with $p < 0.05$ were considered statistically significant.

3. Results

3.1. Changes in body weight, survival rate, and pulmonary function

During the experiment, we monitored the changes in body weight and survival rate, as these parameters can indirectly reflect the health status of mice. At the D35, the mice in the CS + LPS group showed significant decrease in body weight, compared with that of mice in the control and LPS groups (##P < 0.01); however, no significant body weight changes were observed between the CS and CS + LPS groups (Fig. 2A). We also monitored the survival rate weekly and found that the survival rate in the CS + LPS group (80%) was lower than that in the C group (100%), CS group (100%), and LPS group (100%); however, the differences were not statistically significant (Fig. 2B).

Next, we assessed the changes in lung function in terms of Cdyn and RL. Cdyn reflects the change in pulmonary elastic resistance and is used in assessing various types of lung diseases such as pulmonary fibrosis and pleural fibrosis. In contrast, RL can better reflect the airway obstruction and bronchial asthma, emphysema, and obstructive ventilation dysfunction cause increased airway resistance. Our study suggested that the RL of mice from the CS + LPS group was significantly higher than that of mice from the control group (Fig. 2C), and the Cdyn of mice from CS + LPS group was lower than that of mice from the control group (Fig. 2D); however, no significant difference was observed in the Cdyn and RL of mice from the CS + LPS group and the CS or LPS groups. Overall, cigarette smoke exposure combined with LPS-induced lung function changes in mice corresponded to clinical pulmonary fibrosis.

Table 4
Primers sequence for RT-qPCR.

Gene	Forward primer	Reverse primer
β-actin	GGCTGTATTCCCCTCCAT	CCAGTTGGTAACAATGCCATGT
Il-1β	GCCCATCCTCTGTGACTCAT	AGGCCACAGGTATTTTGTCG
TNF-α	ACAGCAAGGGACTAGCCAGGAG	GGAGTGCCTCTTCTGCCAGTT
IL-6	AGTTGCCTTCTTGGGACTGA	TCCACGATTTCCCAGAGAAC
Collagen III	GCTCCTCTTAGGGGCCACT	CCACGTCTCACCATTGGGG
TGF-β	TCAGACATTCGGGAAGCAGT	GCTAAAGCCCTGTATTCCGT
α-SMA	CTTCGCTGGTGATGATGCTC	GTTGGTGATGATGCCGTGTT

3.2. Histopathology of the lung tissues

We examined the histopathology of lung tissues after the third and fifth week. After 3 weeks, smoke exposure alone, LPS administration alone, or CS exposure combined with LPS administration resulted in a certain degree of disorder in the alveolar structure and caused alveolar sepal thickening (Fig. 3A, B). Inflammation scores between the groups were not significantly different (Fig. 3E). After 5 weeks, the CS and LPS groups showed damage and disorder in a small part of the alveolar structure, infiltration of inflammatory cells, and further thickening of alveolar intervals. In the CS + LPS group, the alveolar cavities were damaged or disappeared in most regions of the lung tissue, and the alveolar sepal thickened significantly, inflammatory cell infiltration increased, fibroblast proliferation resulting in the formation of fibrotic lesions, and the inflammation score was significantly increased, compared with the normal group (Fig. 3C, D, F). Overall, cigarette smoke exposure combined with LPS instillation caused severe damage to the lung structure and resulted in formation of fibrotic foci.

3.3. Collagen deposition in mouse lung tissues

Increased collagen deposition in the lung is a characteristic marker of lung fibrosis. Therefore, we used Masson's trichrome staining to evaluate collagen deposition in the lung tissues of mice exposed to CS for 3 weeks (Fig. 4A, B) and 5 weeks (Fig. 4C, D). High amount of collagen deposition was observed in the lung tissues of mice from the CS + LPS group, compared with that of mice from the other groups, and the collagen deposition was more obvious at 5 weeks than at 3 weeks. Furthermore, Ashcroft scores showed that the degree of fibrosis was severe in the CS + LPS group, compared with that in the control group (Fig. 4E, F). As hydroxyproline can indirectly reflect the content of collagen, we also measured the hydroxyproline content in the lung tissues of mice exposed to CS for 5 weeks. The hydroxyproline content in the CS + LPS group was significantly higher than that in the other three groups (Fig. 4G). Moreover, the protein expression and mRNA expression of type III collagen in the lung tissues of the CS + LPS group was significantly higher than that of the control group; however, there was no significant difference compared with the CS and LPS groups (Fig. 4H, I). Thus, cigarette smoke exposure combined with LPS instillation increased the secretion and deposition of collagen in lung tissues, which is an important indicator of pulmonary fibrosis.

3.4. Production of inflammatory cytokines in mouse lung tissues

We measured the levels of IL-1β, TNF-α, and IL-6 in the supernatants of lung tissue homogenates. The levels of TNF-α (Fig. 5A), IL-1β (Fig. 5C), and IL-6 (Fig. 5E) in the CS + LPS group were significantly higher than those in the control group. Moreover, the mRNA expression of IL-1β, TNF-α, and IL-6 in the lung tissues of CS + LPS mice were also found to be increased (Fig. 5B, D, F). Overall, the inflammatory response was enhanced in the CS + LPS group of mice.

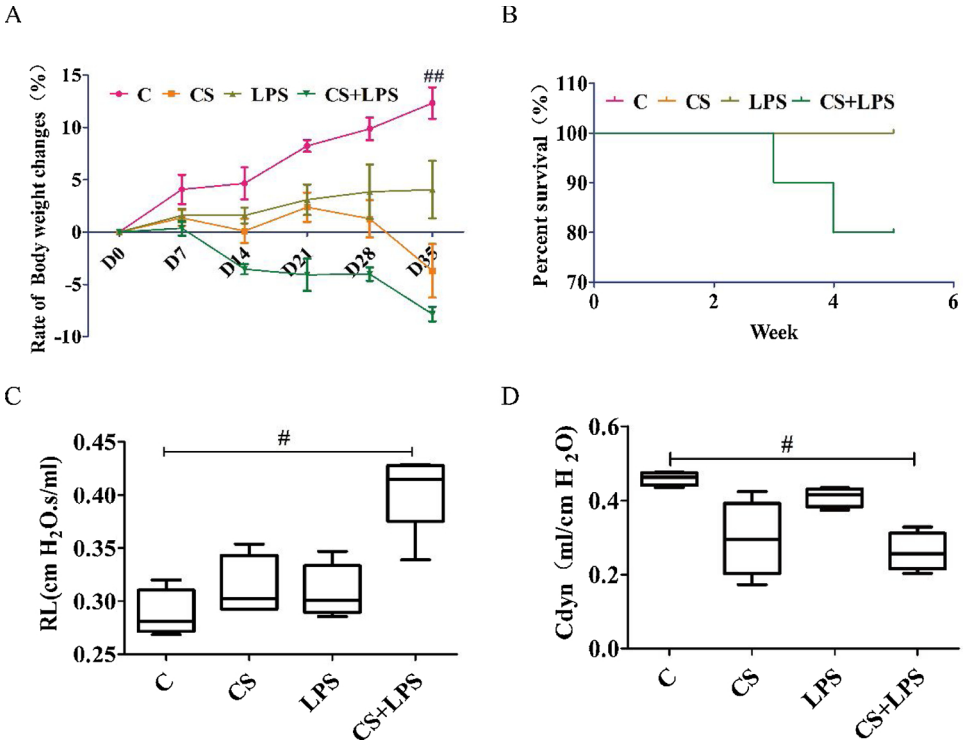

Fig. 2. Changes in body weight, survival rate, and lung function of mice exposed to cigarette smoke (CS) and lipopolysaccharide (LPS) instillation for 5 weeks. At D35, the body weights of mice exposed CS + LPS were significantly decreased (A). Survival rate in the CS + LPS group (80%) was lower than that in the C group (100%), CS group (100%), and LPS group (100%) (B). Dynamic lung compliance (Cdyn) and airway respiratory resistance (RL) were tested using the Buxco system. A significant increase in RL (C) and significant decrease in Cdyn (D) was observed in the CS + LPS group, compared with the control group. Data were presented as median and inter-quartile range, and a nonparametric test (Kruskal-Wallis test) was used for statistical analysis; n = 4–10; #P < 0.05, ##P < 0.01 vs control group.

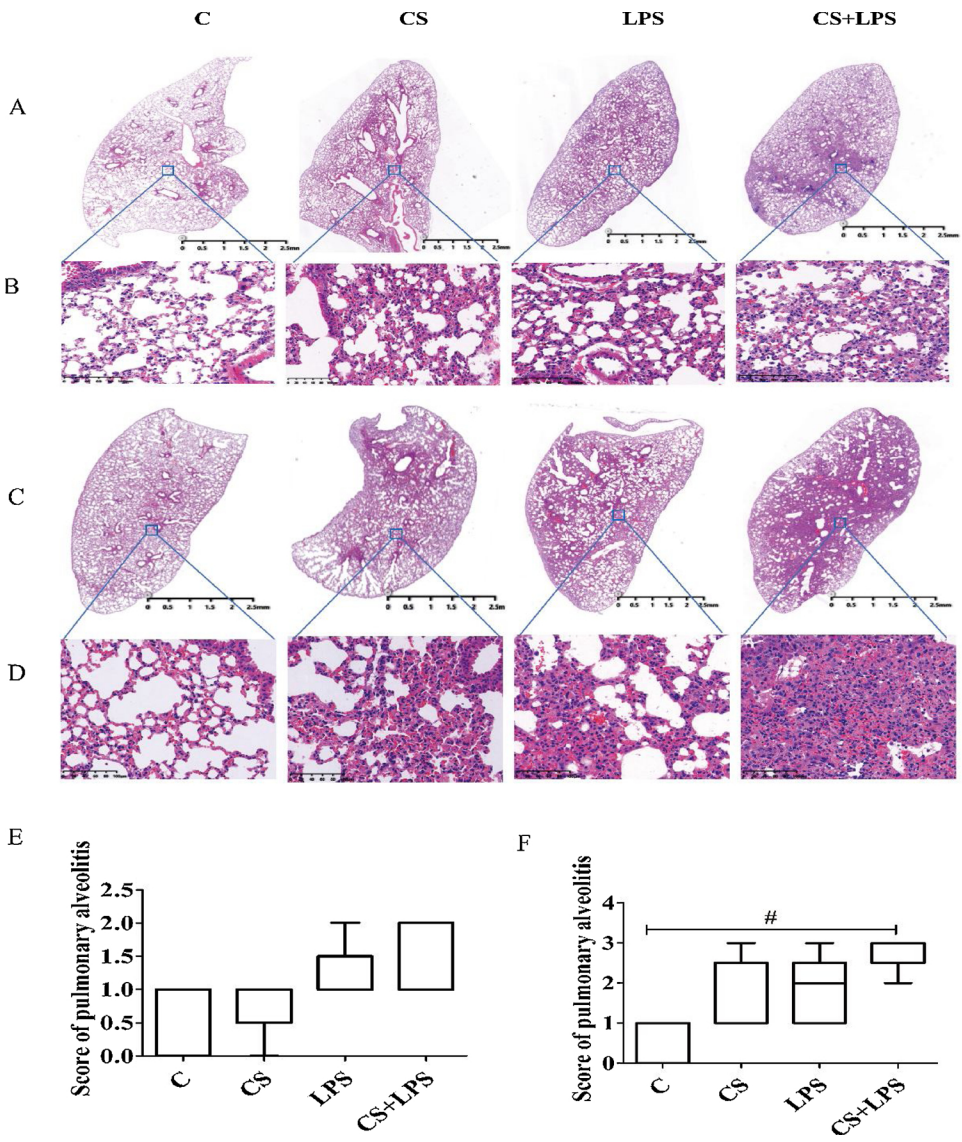

Fig. 3. Haematoxylin and eosin-stained lung histology images from mice exposed to cigarette smoke (CS) and lipopolysaccharide (LPS) instillation. The lung tissues of mice were harvested, and the degree of alveolar inflammation was evaluated in the third week(A, B, E) and the fifth week (C, D, F). The alveolar structure damage and inflammatory cell infiltration were severe in the CS + LPS mice with prolonged exposure to smoke, whereas the CS and LPS groups showed only mild alveolar structure destruction and inflammatory cell infiltration. Representative images of each group have been shown at a magnification of 200X (B, D) or 1X (A, C). Data were presented as median and inter-quartile range, and a nonparametric test (Kruskal-Wallis test) was used for statistical analysis; n = 4–10; #P < 0.05.

3.5. Expression of TGF-β and α-SMA in mouse lung tissues

TGF-β and α-SMA are relevant factors associated with the development of fibrosis. TGF-β is an important factor in the promotion of fibrosis and α-SMA is involved in fibroblast transdifferentiation. We found that the protein and mRNA expression of TGF-β and α-SMA in the lung tissues from the CS + LPS group were significantly higher than those in the control group but did not differ significantly from those of the other groups (Fig. 6A–D). Moreover, immunohistochemistry analysis revealed an increased expression of α-SMA, especially in tissues around the airway and the fibrotic lesions (Fig. 6E, F).

4. Discussion

Smoking is a risk factor for pulmonary fibrosis (Liu et al., 2016), and LPS is a common infectious factor (Thorn, 2001). Therefore, in this study, we investigated whether systemic exposure to cigarette smoke combined with LPS administration can induce pulmonary fibrosis in mice. We found marked alveolar structural disorders, fibrotic lesion formation, and collagen deposition in the lung tissues of mice exposed to CS and subjected to LPS administration. The levels of cytokines such as IL-1β, TNF-α, and IL-6 were also increased in the lung tissues of these mice. Furthermore, lung function analysis revealed significant increase in airway respiratory resistance and a sharp decline in dynamic lung compliance in mice exposed to cigarette smoke and subjected to LPS administration. Overall, this study successfully induced pulmonary fibrosis in mice by CS exposure combined with LPS application, and the resultant pathophysiology was more consistent with that of human pulmonary fibrosis.

Previous studies have shown that intermittent intraperitoneal injection of 5 mg/kg LPS for 3 consecutive days led to endotoxin-induced acute lung injury and fibrosis in mice with the fourth week being the peak period of fibrosis (He et al., 2010). In the present study, we used an LPS concentration of 0.9 mg/kg, and the mice were intermittently (week 2, week 3, week 4) administered intratracheal LPS injections, thereby resulting in minor damage only. This indicates that LPS alone did not result in lesion formation and that smoke exposure may play an important role in lesion formation.

A previous study has shown that cigarette smoke aggravates the severity of acute lung injury caused by LPS and that lung IL-6, which is significantly higher in LPS-injured mice previously exposed to cigarette smoke, may be considered as a tobacco-related lung injury biomarker (Gotts et al., 2017). The results of our study are consistent with this previous result, as we found significantly high IL-6 levels in the CS + LPS group. Furthermore, exposure to cigarette smoke in guinea pigs has been reported to aggravate pulmonary fibrosis caused by bleomycin,

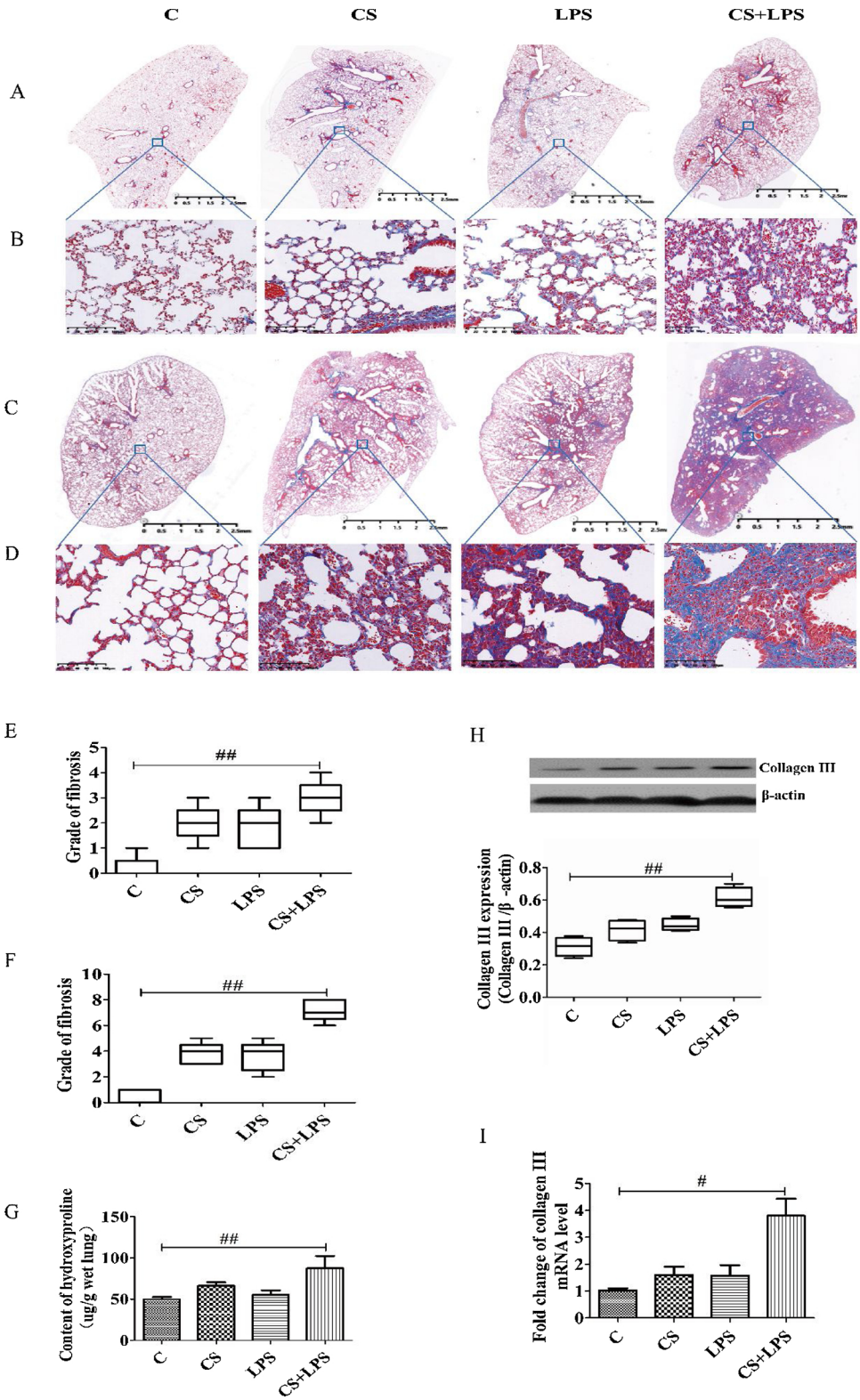

Fig. 4. Collagen deposition in the lung tissues of mice. The degree of collagen deposition was assessed by Masson's trichrome staining. The lung tissues of mice were harvested after the third week(A, B)and the fifth week (C,D). Ashcroft score was used to evaluate the degree of fibrosis in the third week (E) and fifth week (F). Hydroxyproline content in lung was measured by the hydroxyproline assay (G). Expression of collagen III in the lung was measured by western blot (H) and reverse transcription-quantitative polymerase chain reaction (RT-qPCR) (I). Mice in CS + LPS group showed significantly increased collagen deposition and severe fibrosis. Representative images of each group have been shown at a magnification of 200X (B, D) or 1X (A, C). Data were presented as median and inter-quartile range, and a nonparametric test (Kruskal-Wallis test) was used for statistical analysis (E, F, H); data were presented as mean ± SEM, and a parametric test (one-way ANOVA) was used for statistical analysis (G, I); n = 3–6; #P < 0.05; ##P < 0.01.

suggesting that tobacco smoke creates a profibrotic microenvironment in the lungs (Cisneros-Lira et al., 2003).

Alveolar epithelial injury is one of the pathogenesis mechanisms of pulmonary fibrosis (Sisson et al., 2010; King et al., 2011). Cigarette smoke has a complex composition, and it contains several strong oxidants that generate reactive oxygen species (ROS) via a series of reactions (Pryor and Stone, 1993; Jiao et al., 2006). The damage to alveolar type II epithelial cell (AECII) is mainly mediated by oxidative stress (Faux et al., 2009) resulting from ROS accumulation.

Oxidative stress can damage cellular lipids, sugars, proteins, and DNA via ROS, thus causing cell damage (Bargagli et al., 2009). A previous study on the role of cigarette smoke-induced oxidative stress in AECII injury, showed that the combined effect of oxidative stress and inflammatory response is one of the mechanisms underlying AECII damage. Numerous other studies showed that oxidative stress and inflammatory response form a vicious circle. Oxidative stress promotes

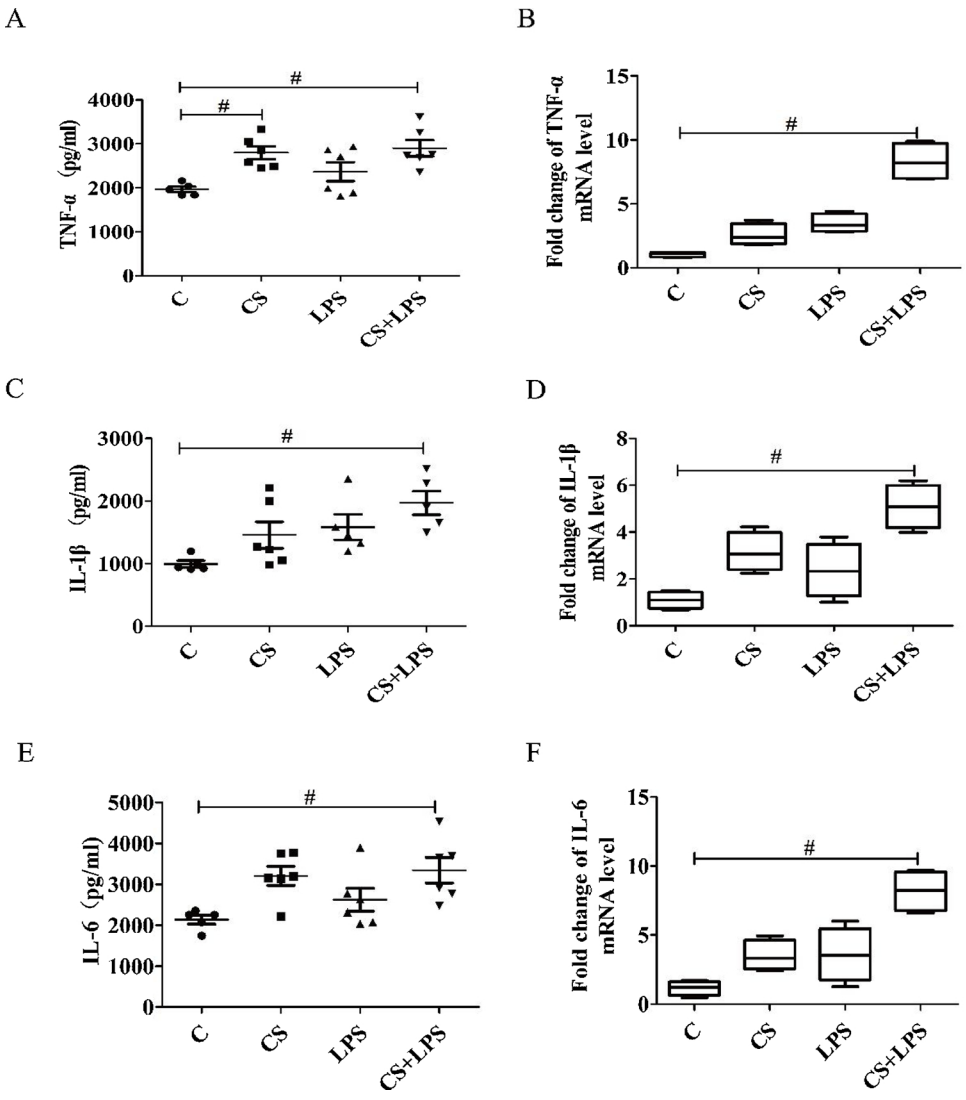

Fig. 5. Production of cytokines in lung tissue after cigarette smoke exposure (CS) and lipopolysaccharide (LPS) instillation. The levels of IL-1β, TNF-α, and IL-6 in lung tissue homogenates were quantified by ELISA (A, C, E) and reverse transcription-quantitative polymerase chain reaction (RT-qPCR) (B, D, E). IL-6, IL-1β, and TNF-α levels in the CS + LPS group were significantly higher than those in the control group. Data were presented as median and inter-quartile range, and a nonparametric test (Kruskal-Wallis test) was used for statistical analysis (B, D, F); data were presented as mean ± SEM, and a parametric test (one-way ANOVA) was used for statistical analysis (A, C, E); n = 3–6; #P < 0.05; ##P < 0.01.

the expression of inflammatory factors by activating certain kinases or transcription factors such as nuclear factor-kappa B (NF-κB) and activator protein 1 (AP-1) (Rahman and Adcock, 2006), thereby aggravating the inflammatory response. In contrast, the inflammatory mediators such as IL-1, IL-6, and TNF-α can stimulate the release of ROS and intensify oxidative stress (Thannickal and Fanburg, 2000; Park et al., 2009). In our study, the expression of IL-6 and TNF-α in lung tissues was increased, suggesting that the pathological changes in pulmonary fibrosis are related to alveolar epithelial injury caused by cigarette smoke-induced oxidative stress.

In order to elucidate the pathogenesis of pulmonary fibrosis and identify effective treatment methods, animal models of pulmonary fibrosis have been established using hyperoxia (Chen et al., 2014), irradiation (McDonald et al., 1993), silica dust (Fazzi et al., 2014), bleomycin (Mouratis and Aidinis, 2011), paraquat (Greenberg et al., 1978), and fluorescein isothiocyanate (Roberts et al., 1995). Hyperoxia-induced pulmonary fibrosis model is mainly used to simulate acute lung injury and pulmonary fibrosis caused by clinical oxygen therapy. Irradiation-induced pulmonary fibrosis model can accurately imitate the pathophysiological changes of pulmonary fibrosis caused by exposure to radioactive sources in clinical practice; however, developing this model is time consuming (20–30 weeks) and expensive. Silica-induced pulmonary fibrosis models can be developed in 12–16 weeks; however, Balb/c mice are resistant and special equipment is needed for aerosol-based delivery. Bleomycin-induced pulmonary fibrosis is reported to be self-limiting after 28 days and development of fibrosis is limited in Balb/c mice. Lung injury caused by paraquat poisoning usually occurs within 5–9 days after poisoning and reaches its peak within 2–3 weeks; the disease is severe and progresses rapidly. In the fluorescein isothiocyanate-induced models, the response can vary depending on lot of the fluorescein isothiocyanate, and the model is not clinically relevant. As the pathological process of human pulmonary fibrosis is complex, and the formation and development of this disease is affected by genetic, biochemical, and environmental factors, animal models cannot fully simulate the process of human pulmonary fibrosis. In our study, smoking, a behaviour closely related to human lifestyle, was used to induce pulmonary fibrosis. Subsequent LPS stimulation during CS exposure accelerated the inflammatory response and fibrosis progression. Therefore, the resulting pathophysiological changes observed in these mouse models are more consistent with those in human pulmonary fibrosis. Therefore, this method serves as a better approach to develop animal models for investigating the mechanisms underlying the pathogenesis of pulmonary fibrosis as well as for identifying and testing novel clinical treatments for pulmonary fibrosis.

In this study, we successfully induced pathological changes manifested in pulmonary fibrosis in mice. This study may serve as a foundation for the creation of new animal models for pulmonary fibrosis and help to improve the diagnosis of clinical pulmonary fibrosis. However, we did not investigate the dynamic changes during the development of such models and the underlying mechanisms; for example, the

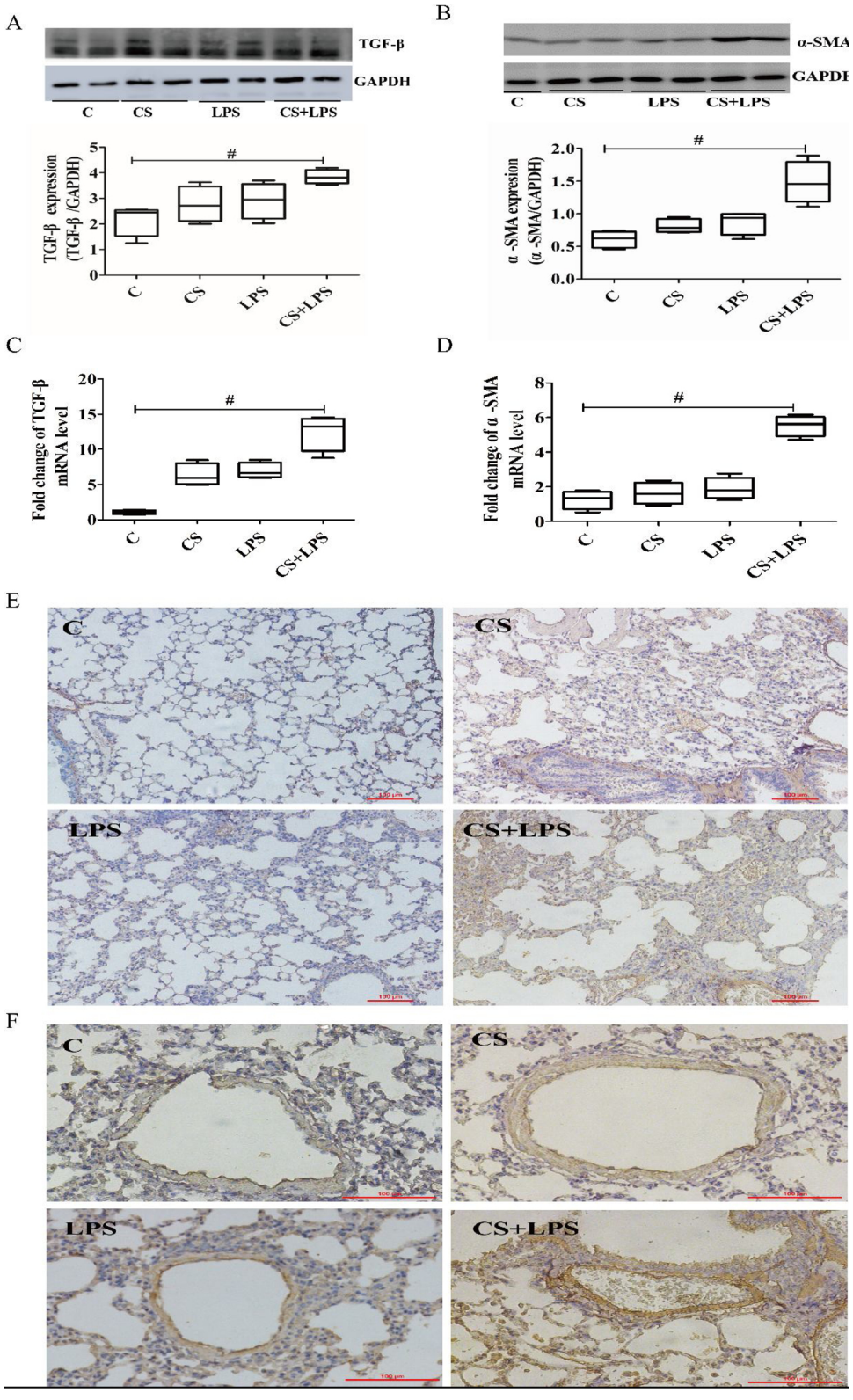

Fig. 6. Expression of TGF-β and α-SMA in the lung tissues of mice exposed to cigarette smoke and lipopolysaccharide instillation (CS + LPS). The protein and mRNA expression of TGF-β and α-SMA was quantified by western blot and RT-qPCR respectively (A–D). α-SMA expression in the lung tissues was detected by immunohistochemistry. α-SMA expression in the airway and fibrotic lesion areas was increased in mice of the CS + LPS group compared to control group. (E, F). Representative images of each group have been shown at a magnification of 100X (E) or 200X (F). Data were presented as median and inter-quartile range, and a nonparametric test (Kruskal-Wallis test) was used for statistical analysis; n = 3–6; #P < 0.05; ##P < 0.01.

pathological changes in pulmonary fibrosis may be related to alveolar epithelial injury caused by cigarette smoke-induced oxidative stress. Thus, further studies are warranted to investigate these aspects.

5. Conclusions

This study indicates that cigarette exposure and LPS-induced lung injury induce pulmonary fibrosis in mice. It leads to alveolar structural disorders, fibrotic lesion formation, collagen deposition, increased inflammatory cytokine levels, increased airway respiratory resistance, and declined dynamic lung compliance in the lung tissues of mice. Overall, this study successfully developed mouse pulmonary fibrosis models with pathophysiology highly similar to that observed in human pulmonary fibrosis.

Competing interests

The authors have no competing interests to declare.

Acknowledgments

This work was supported by the National Natural Science Foundation of China (grant numbers: 81170717, 81570065), the Natural Science Foundation of Hunan Province (grant number: 2017JJ2400), the innovation Foundation of Hunan Province Education Department (grant number: 17K101), Fundamental Research Funds for the Central Universities of Central South University Grant (grant number: 2018zzts039, 2018zzts816), and the fund for the key laboratory of Hunan province (grant number: 2017TP1004).

References

Akhmetshina, A., Palumbo, K., Dees, C., Bergmann, C., Venalis, P., Zerr, P., Horn, A., Kireva, T., Beyer, C., Zwerina, J., Schneider, H., 2012. Activation of canonical Wnt signalling is required for TGF-β-mediated fibrosis. Nat. Commun. 3, 735. https://doi.org/10.1038/ncomms1734.

Ashcroft, T., Simpson, J.M., Timbrell, V., 1988. Simple method of estimating severity of pulmonary fibrosis on a numerical scale. J. Clin. Pathol. 41, 467–470. https://doi.org/10.1136/jcp.41.4.467.

Bargagli, E., Olivieri, C., Bennett, D., Prasse, A., Muller-Quernheim, J., Rottoli, P., 2009. Oxidative stress in the pathogenesis of diffuse lung diseases: a review. Respir. Med. 103, 1245–1256. https://doi.org/10.1016/j.rmed.2009.04.014.

Baumgartner, K.B., Samet, J.M., Stidley, C.A., Colby, T.V., Waldron, J.A., 1997. Cigarette smoking: a risk factor for idiopathic pulmonary fibrosis. Am. J. Respir. Crit. Care Med. 155, 242–248. https://doi.org/10.1164/ajrccm.155.1.9001319.

Chen, H.L., Yen, C.C., Wang, S.M., Tsai, T.C., Lai, Z.L., Sun, J.Y., Lin, W., Hsu, W.H., Chen, C.M., 2014. Aerosolized bovine lactoferrin reduces lung injury and fibrosis in mice exposed to hyperoxia. Biometals 27, 1057–1068. https://doi.org/10.1007/s10534-014-9750-7.

Cisneros-Lira, J., Gaxiola, M., Ramos, C., Selman, M., Pardo, A., 2003. Cigarette smoke exposure potentiates bleomycin-induced lung fibrosis in guinea pigs. Am. J. Physiol. Lung Cell Mol. Physiol. 285, L949–L956. https://doi.org/10.1152/ajplung.00074.2003.

Cottin, V., Nunes, H., Brillet, P.Y., Delaval, P., Devouassoux, G., Tillie-Leblond, I., Israel-Biet, D., Valeyre, D., Cordier, J.F., 2005. Combined pulmonary fibrosis and emphysema: a distinct underrecognised entity. Eur. Respir. J. 26, 586–593. https://doi.org/10.1183/09031936.05.00021005.

Dohi, M., Hasegawa, T., Yamamoto, K., Marshall, B.C., 2000. Hepatocyte growth factor attenuates collagen accumulation in a murine model of pulmonary fibrosis. Am. J. Respir. Crit. Care Med. 162, 2302–2307. https://doi.org/10.1164/ajrccm.162.6.9908097.

Faux, S.P., Tai, T., Thorne, D., Xu, Y., Breheny, D., Gaca, M., 2009. The role of oxidative stress in the biological responses of lung epithelial cells to cigarette smoke. Biomarkers 14, 90–96. https://doi.org/10.1080/13547500902965047.

Fazzi, F., Njah, J., Di Giuseppe, M., Winnica, D.E., Go, K., Sala, E., St Croix, C.M., Watkins, S.C., Tyurin, V.A., Phinney, D.G., Fattman, C.L., 2014. TNFR1/phox interaction and TNFR1 mitochondrial translocation Thwart silica-induced pulmonary fibrosis. J. Immunol. 192, 3837–3846. https://doi.org/10.4049/jimmunol.1103516.

Gotts, J.E., Abbott, J., Fang, X., Yanagisawa, H., Takasaka, N., Nishimura, S.L., Calfee, C.S., Matthay, M.A., 2017. Cigarette smoke exposure worsens endotoxin-induced lung injury and pulmonary edema in mice. Nicotine Tob. Res. 19, 1033–1039. https://doi.org/10.1093/ntr/ntx062.

Greenberg, D.B., Reiser, K.M., Last, J.A., 1978. Correlation of biochemical and morphologic manifestations of acute pulmonary fibrosis in rats administered paraquat. Chest 74, 421–425. https://doi.org/10.1016/S0012-3692(15)37391-8.

Grubstein, A., Bendayan, D., Schactman, I., Cohen, M., Shitrit, D., Kramer, M.R., 2005. Concomitant upper-lobe bullous emphysema, lower-lobe interstitial fibrosis and pulmonary hypertension in heavy smokers: report of eight cases and review of the literature. Respir. Med. 99, 948–954. https://doi.org/10.1016/j.rmed.2004.12.010.

He, Z., Zhu, Y., Jiang, H., 2009. Toll-like receptor 4 mediates lipopolysaccharide-induced collagen secretion by phosphoinositide3-kinase- akt pathway in fibroblasts during acute lung injury. J. Recept. Signal Transduct. Res. 29, 119–125. https://doi.org/10.1080/10799890902845690.

He, Z., Zhu, Y., Jiang, H., 2010. Establishing a mouse model of acute lung injury and pulmonary fibrosis by intermittent lipopolysaccharide intraperitoneal injection. Chin. J. Respir. Crit. Care 9, 76–80.

Jensen, K., Nizamutdinov, D., Guerrier, M., Afroze, S., Dostal, D., Glaser, S., 2012. General mechanisms of nicotine-induced fibrogenesis. FASEB J. 26, 4778–4787. https://doi.org/10.1096/fj.12-206458.

Jiao, Z.X., Ao, Q.L., Xiong, M., 2006. Cigarette smoke extract inhibits the proliferation of alveolar epithelial cells and induces apoptosis. Acta Phys. Chim. Sin. 58, 244–254. https://doi.org/10.1007/s11596-008-0102-0.

King Jr., T.E., Pardo, A., Selman, M., 2011. Idiopathic pulmonary fibrosis. Lancet 378, 1949–1961. https://doi.org/10.1016/S0140-6736(11)60052-4.

Li, H., Du, S., Yang, L., Chen, Y., Huang, W., Zhang, R., Cui, Y., Yang, J., Chen, D., Li, Y., Zhang, S., 2009. Rapid pulmonary fibrosis induced by acute lung injury via a lipopolysaccharide three-hit regimen. Innate Immun. 15, 143–154. https://doi.org/10.1177/1753425908101509.

Liu, Y.M., Nepali, K., Liou, J.P., 2016. Idiopathic pulmonary fibrosis: current status, recent progress, and emerging targets. J. Med. Chem. 60, 527–553. https://doi.org/10.1021/acs.jmedchem.6b00935.

Maniatis, N.A., Kotanidou, A., Catravas, J.D., Orfanos, S.E., 2008. Endothelial pathomechanisms in acute lung injury. Vascul. Pharmacol. 49, 119–133. https://doi.org/10.1016/j.vph.2008.06.009.

McDonald, S., Rubin, P., Chang, A.Y., Penney, D.P., Finkelstein, J.N., Grossberg, S., Feins, R., Gregory, P.K., 1993. Pulmonary changes induced by combined mouse beta-interferon (rMuIFN-beta) and irradiation in normal mice—toxic versus protective effects. Radiother. Oncol. 26, 212–218. https://doi.org/10.1016/0167-8140(93)90262-7.

Moore, B.B., Hogaboam, C.M., 2008. Murine models of pulmonary fibrosis. Am. J. Physiol. Lung Cell Mol. Physiol. 294, L152–L160 https://doi.org/10.1152/ajplung.00313.2007.

Mouratis, M.A., Aidinis, V., 2011. Modeling pulmonary fibrosis with bleomycin. Curr. Opin. Pulm. Med. 17, 355–361. https://doi.org/10.1097/MCP.0b013e328349ac2b.

Olman, M.A., White, K.E., Ware, L.B., Simmons, W.L., Benveniste, E.N., Zhu, S., Pugin, J., Matthay, M.A., 2004. Pulmonary edema fluid from patients with early lung injury stimulates fibroblast proliferation through IL-1 beta-induced IL-6 expression. J. Immunol. 172, 2668–2677. https://doi.org/10.4049/jimmunol.172.4.2668.

Park, H.S., Kim, S.R., Lee, Y.C., 2009. Impact of oxidative stress on lung diseases. Respirology 14, 27–38. https://doi.org/10.1111/j.1440-1843.2008.01447.x.

Pryor, W.A., Stone, K., 1993. Oxidants in cigarette smoke. Radicals, hydrogen peroxide, peroxynitrate, and peroxynitrite. Ann. N. Y. Acad. Sci. 686, 12–27. https://doi.org/10.1111/j.1749-6632.1993.tb39148.x.

Raghu, G., Collard, H.R., Egan, J.J., Martinez, F.J., Behr, J., Brown, K.K., Colby, T.V., Cordier, J.F., Flaherty, K.R., Lasky, J.A., Lynch, D.A., 2011. An official ATS/ERS/JRS/ALAT statement: idiopathic pulmonary fibrosis: evidence-based guidelines for diagnosis and management. Am. J. Respir. Crit. Care Med. 183, 788–824. https://doi.org/10.1164/rccm.2009-040GL.

Rahman, I., Adcock, I.M., 2006. Oxidative stress and redox regulation of lung inflammation in COPD. Eur. Respir. J. 28, 219–242. https://doi.org/10.1183/09031936.06.00053805.

Roberts, S.N., Howie, S.E.M., Wallace, W.A.H., Brown, D.M., Lamb, D., Ramage, E.A., Donaldson, K., 1995. A novel model for human interstitial lung disease: hapten-driven lung fibrosis in rodents. J. Pathol. 176, 309–318. https://doi.org/10.1002/path.1711760313.

Roomans, G.M., Vanthanouvong, V., Dragomir, A., Kozlova, I., Wróblewski, R., 2002. Effects of nicotine on intestinal and respiratory epithelium. J. Submicrosc. Cytol. Pathol. 34, 381–388.

Sebai, H., Ben-Attia, M., Sani, M., Aouani, E., Ghanem-Boughanmi, N., 2009. Protective effect of resveratrol in endotoxemia-induced acute phase response in rats. Arch. Toxicol. 83, 335–340. https://doi.org/10.1007/s00204-008-0348-0.

Seki, E., De Minicis, S., Österreicher, C.H., Kluwe, J., Osawa, Y., Brenner, D.A., Schwabe, R.F., 2007. TLR4 enhances TGF-beta signaling and hepatic fibrosis. Nat. Med. 13, 1324–1332. https://doi.org/10.1038/nm1663.

Selman, M., Pardo, A., 2014. Revealing the pathogenic and aging-related mechanisms of the enigmatic idiopathic pulmonary fibrosis. an integral model. Am. J. Respir. Crit. Care Med. 189, 1161–1172. https://doi.org/10.1164/rccm.201312-2221PP.

Sisson, T.H., Mendez, M., Choi, K., Subbotina, N., Courey, A., Cunningham, A., Dave, A., Engelhardt, J.F., Liu, X., White, E.S., Thannickal, V.J., 2010. Targeted injury of type II alveolar epithelial cells induces pulmonary fibrosis. Am. J. Respir. Crit. Care Med. 181, 254–263. https://doi.org/10.1164/rccm.200810-1615OC.

Szapiel, S.V., Elson, N.A., Fulmer, J.D., Hunninghake, G.W., Crystal, R.G., 1979. Bleomycin-induced interstitial pulmonary disease in the nude, athymic mouse. Am. Rev. Respir. Dis. 120, 893–899.

Thannickal, V.J., Fanburg, B.L., 2000. Reactive oxygen species in cell signaling. Am. J. Physiol. Lung Cell Mol. Physiol. 279, L1005–L1028. https://doi.org/10.1152/ajplung.2000.279.6.L1005.

Thorn, J., 2001. The inflammatory response in humans after inhalation of bacterial endotoxin: a review. Inflamm. Res. 50, 254–261. https://doi.org/10.1007/s000110050751.

Vancheri, C., Crimi, N., Conte, E., Pistorio, M.P., Mastruzzo, C., Lamicela, M., Messina, A., Mistretta, A., 1996. Human lung fibroblasts inhibit tumor necrosis factor-alpha production by LPS-activated monocytes. Am. J. Respir. Cell Mol. Biol. 15, 460–466. https://doi.org/10.1165/ajrcmb.15.4.8879179.